Supplementary Materials for

What caused record-breaking aerosol loading over the South China Sea in April 2023

Saginela Ravindra Babu[1*] and Neng-Huei Lin[1,2*]

[1]Department of Atmospheric Sciences, National Central University, Taoyuan 32001, Taiwan.

[2]Center for Environmental Monitoring and Technology, National Central University, Taoyuan 32001, Taiwan.

Correspondence to**:** S. Ravindra Babu (baburavindra595@gmail.com) and Neng-Huei Lin (nhlin@cc.ncu.edu.tw).

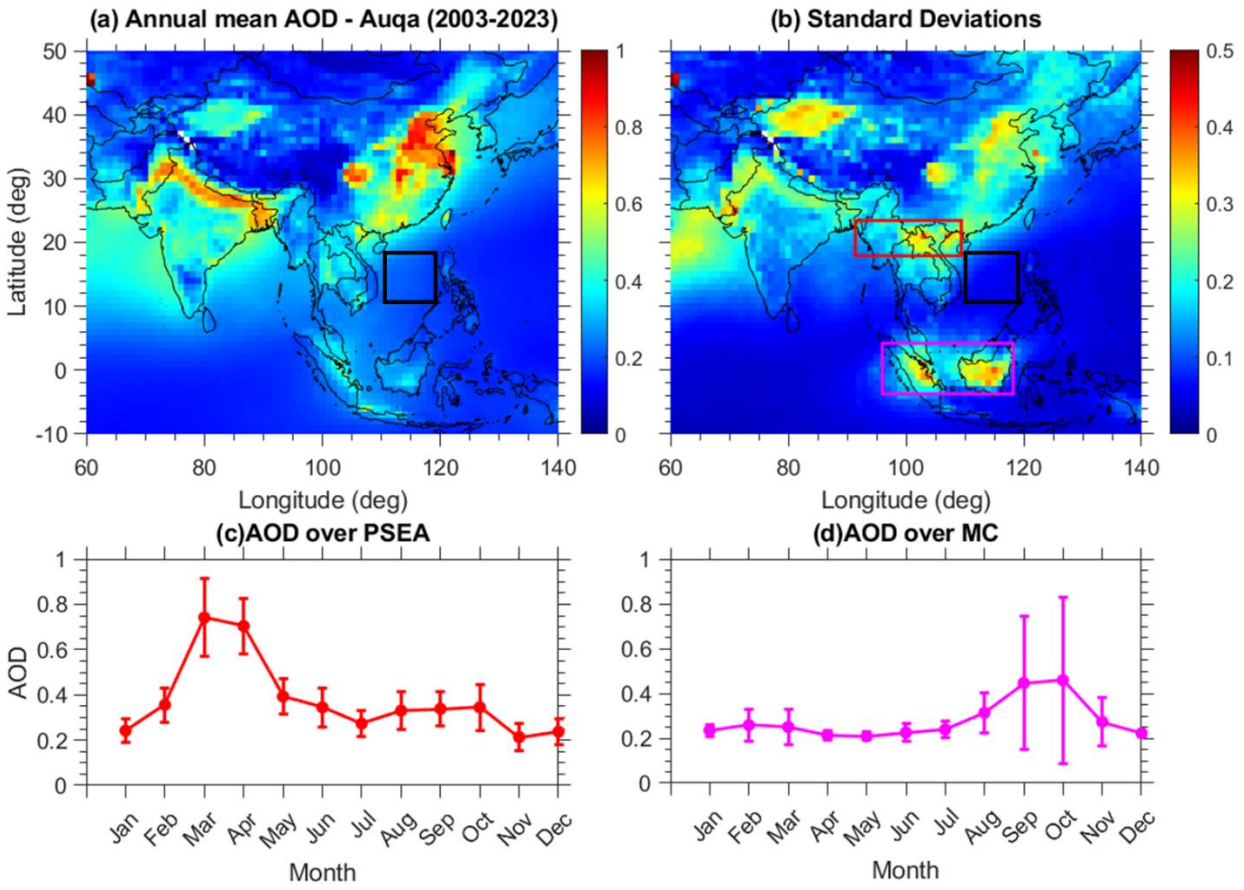

Sup. Figure 1. Climatological mean distribution of MODIS (a) Aerosol Optical Depth (AOD) and (b) respective standard deviations. The black box illustrated in both figures emphasizes the specific area of the South China Sea (SCS) that is the primary focus of this research. (109-119E, 11-18N). The red and magenta boxes indicate the PSEA and MC, which are two significant regions for biomass burning in the vicinity of the SCS. The long-term average seasonal variation in AOD is illustrated over (c) PSEA and (d) MC.

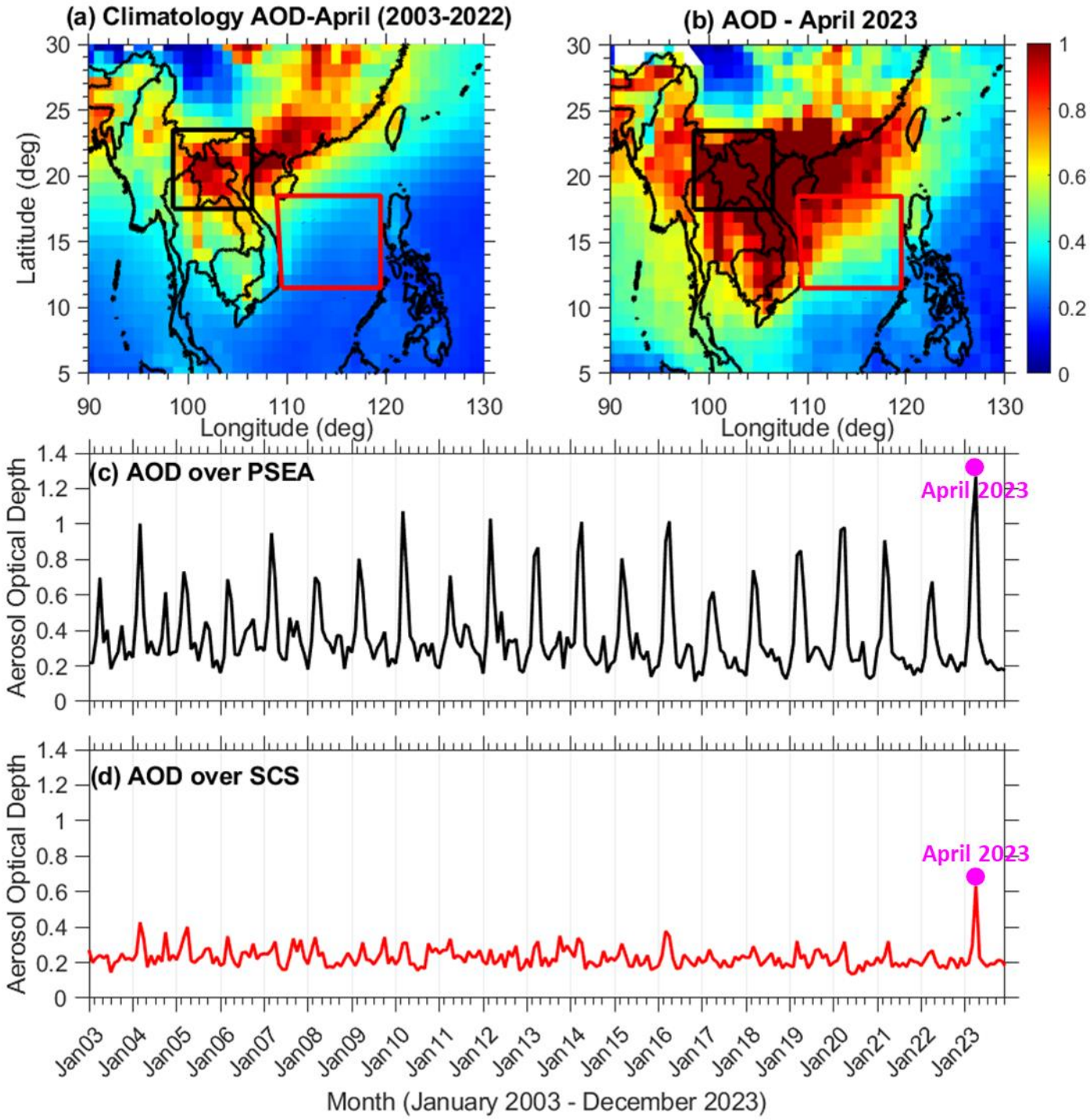

Sup. Figure 2. Spatial distribution of (a) Inter-annual (2003 to 2022) monthly average AOD values for April. (b) Monthly AOD values for April 2023. A notable increase in AOD values is observed over the peninsular Southeast Asia and the South China Sea. (c) Time series of average monthly mean AOD values over the northern Peninsula of Southeast Asia (17-23N, 99- 106E), and (d) over the South China Sea (109-119E, 11-18N) from January 2003 to December 2023. The magenta dot in subplots (c) and (d) marks the AOD values during April 2023. AOD distribution averaged in

April over the past two decades indicated a belt region with high aerosol loading, extending from northern Laos to the southern coast of China. During April 2023, extreme AOD values were observed across the entire PSEA, extending to coastal South China and the South China Sea.

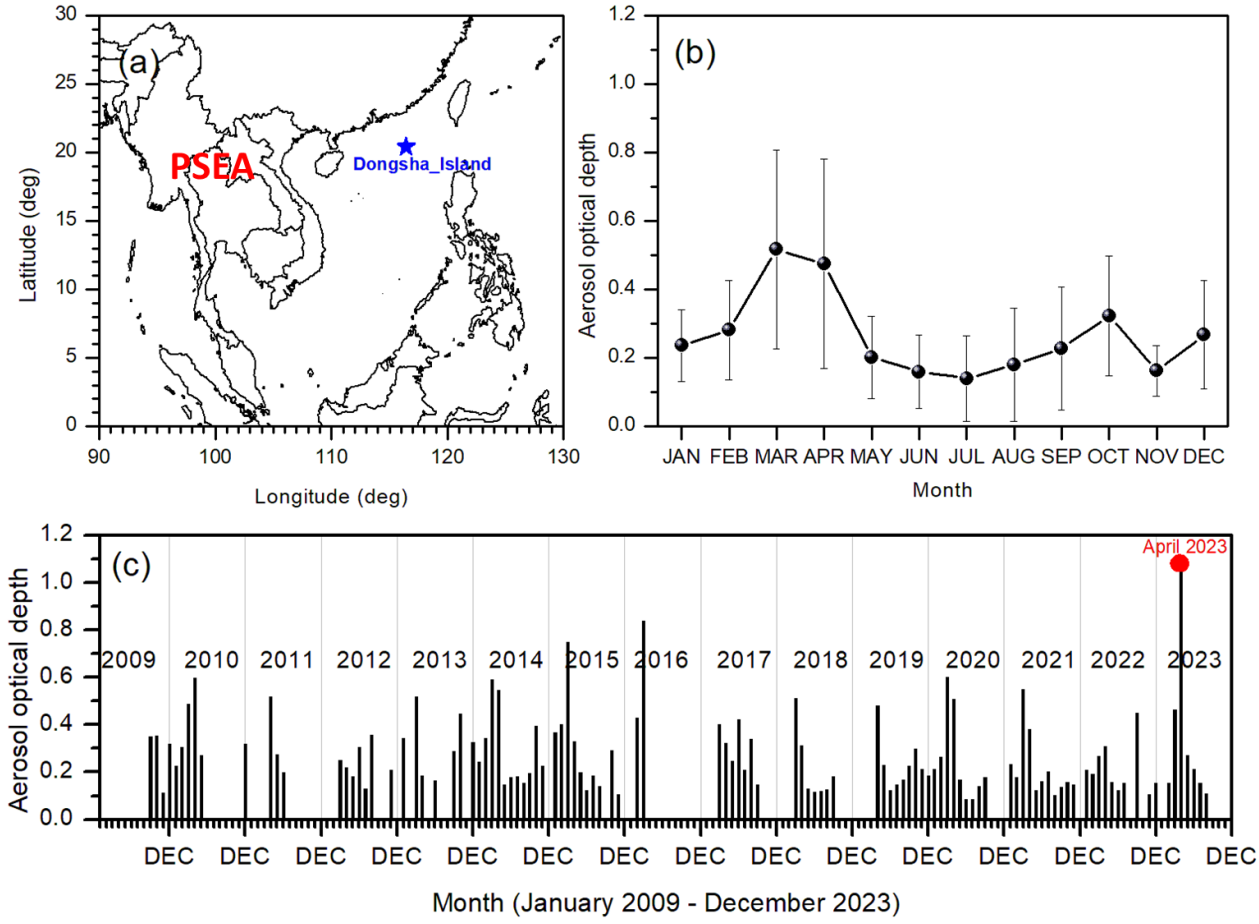

Sup. Figure 3. The location of the Dongsha_Island (20.70°N, 116.73°E, 5 m a.s.l.) AERONET site (denoted by the blue star) in the South China Sea. (b) Monthly variations in aerosol optical depth (AOD) at Dongsha. Vertical error bars represent the standard deviation from the mean. (c) Time series of monthly AOD values from January 2009 to December 2023. The highest AOD occurred in April 2023, marking the peak of the entire data period.

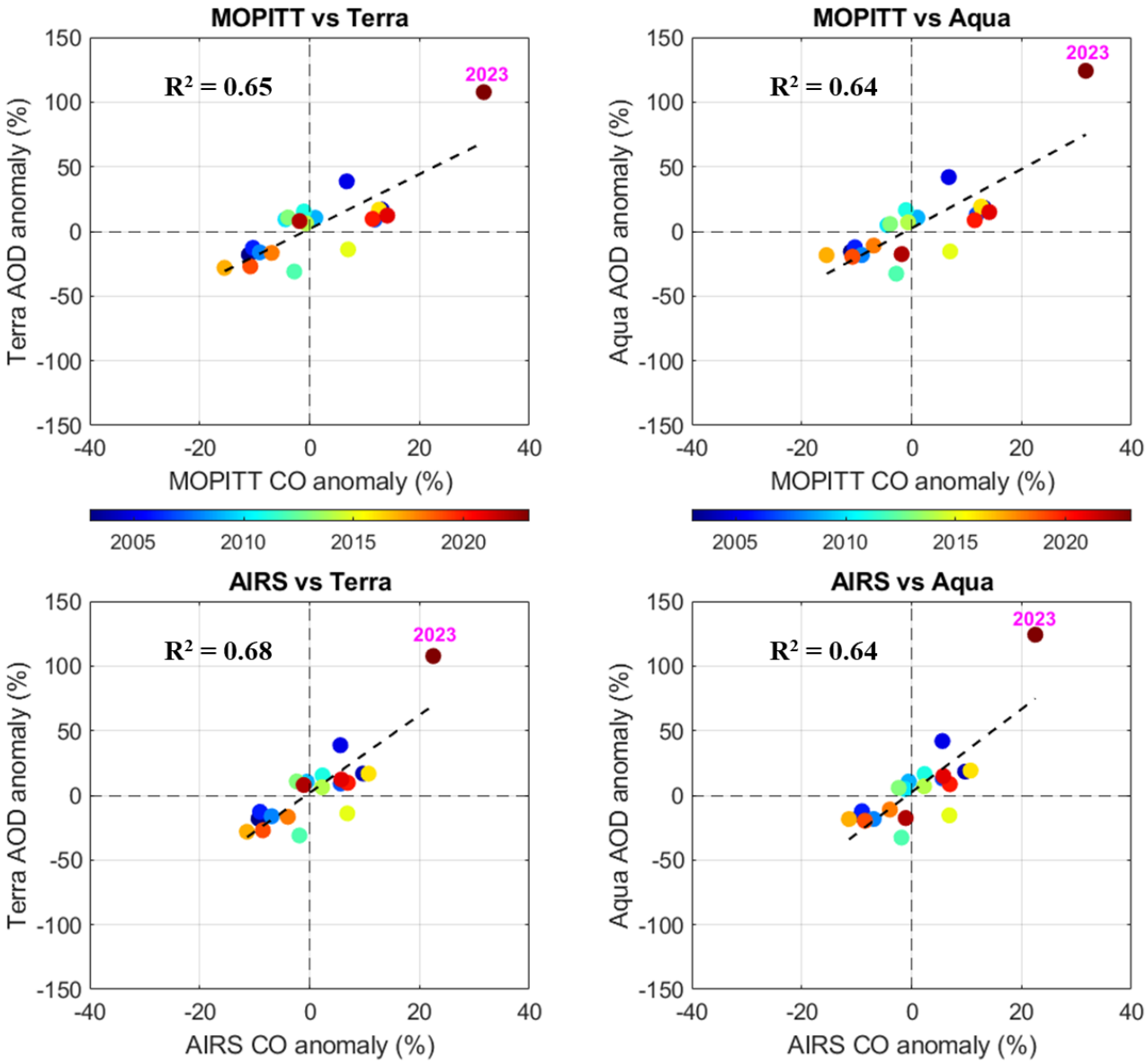

Sup. Figure 4. Bubble plot of the AOD and CO anomalies (April) over the South China Sea (10.5–18.5°N, 109.5–119.5°E) during 2003–2023. To panels for MOPITT and MODIS (Terra and Aqua), whereas the bottom panels are for AIRS and MODIS observations.

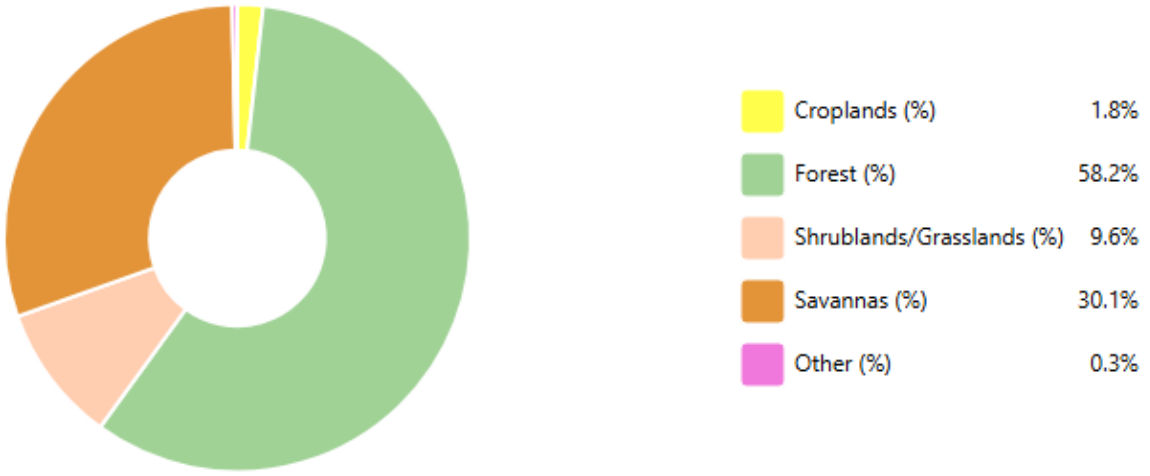

Sup. Figure 5. Distribution of land cover types over Laos. (Source: taken from https://gwis.jrc.ec.europa.eu/apps/country.profile/).

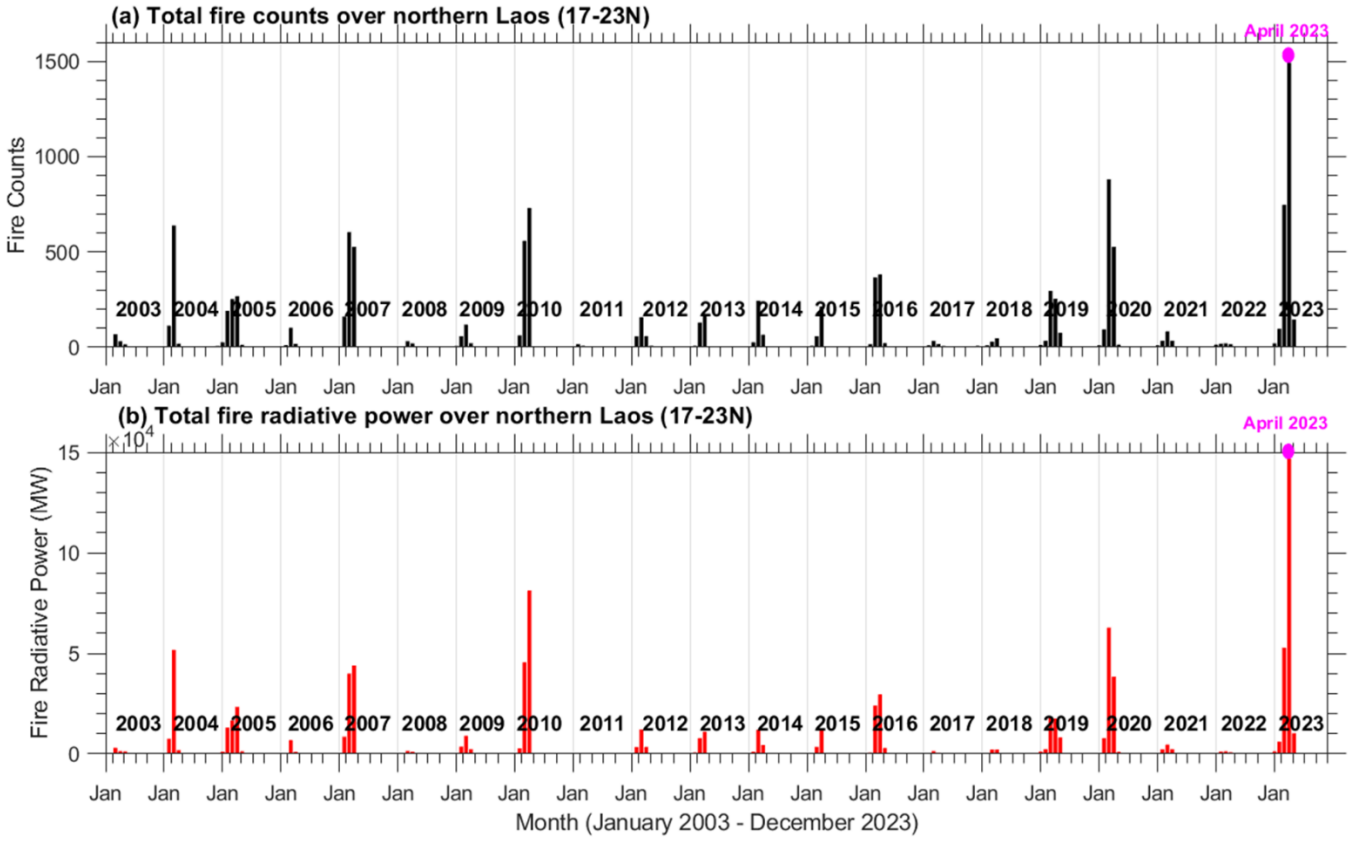

Sup. Figure 6. Inter-annual monthly nighttime (a) total fire counts and (b) the total fire radiative power (FRP) over northern Laos from January 2003 to December 2023.

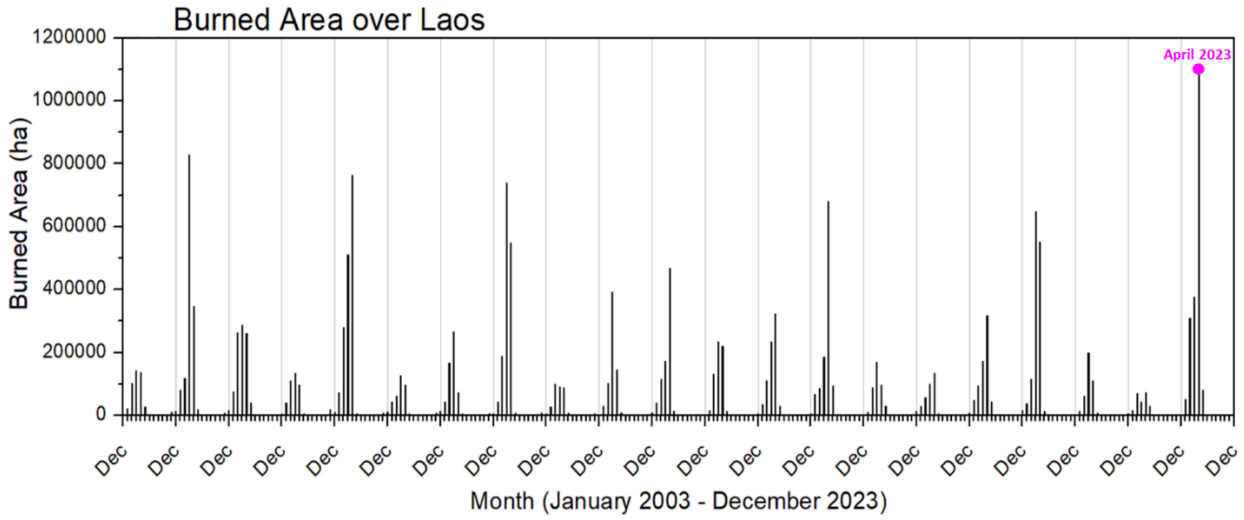

Sup. Figure 7. Time series of MODIS monthly total burned area (BA) values over Laos from January 2003 to December 2023. The most significant area burned in a single month on recent record (2002-2023) occurred in April 2023 with 1.08 Mha burned.

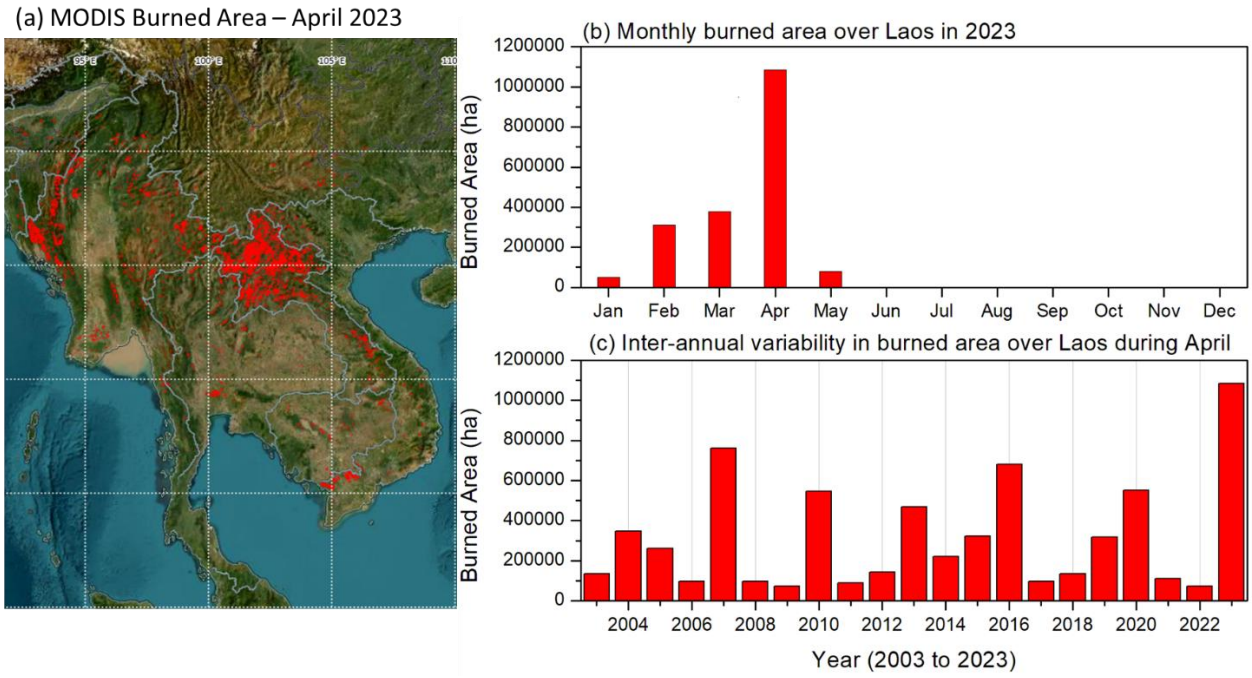

Sup. Figure 8. (a) The spatial distribution of MODIS burned area (BA) in April 2023, (b) MODIS monthly total burned area variability in 2023, (c) the observed inter-annual variability in BA for April over Laos.

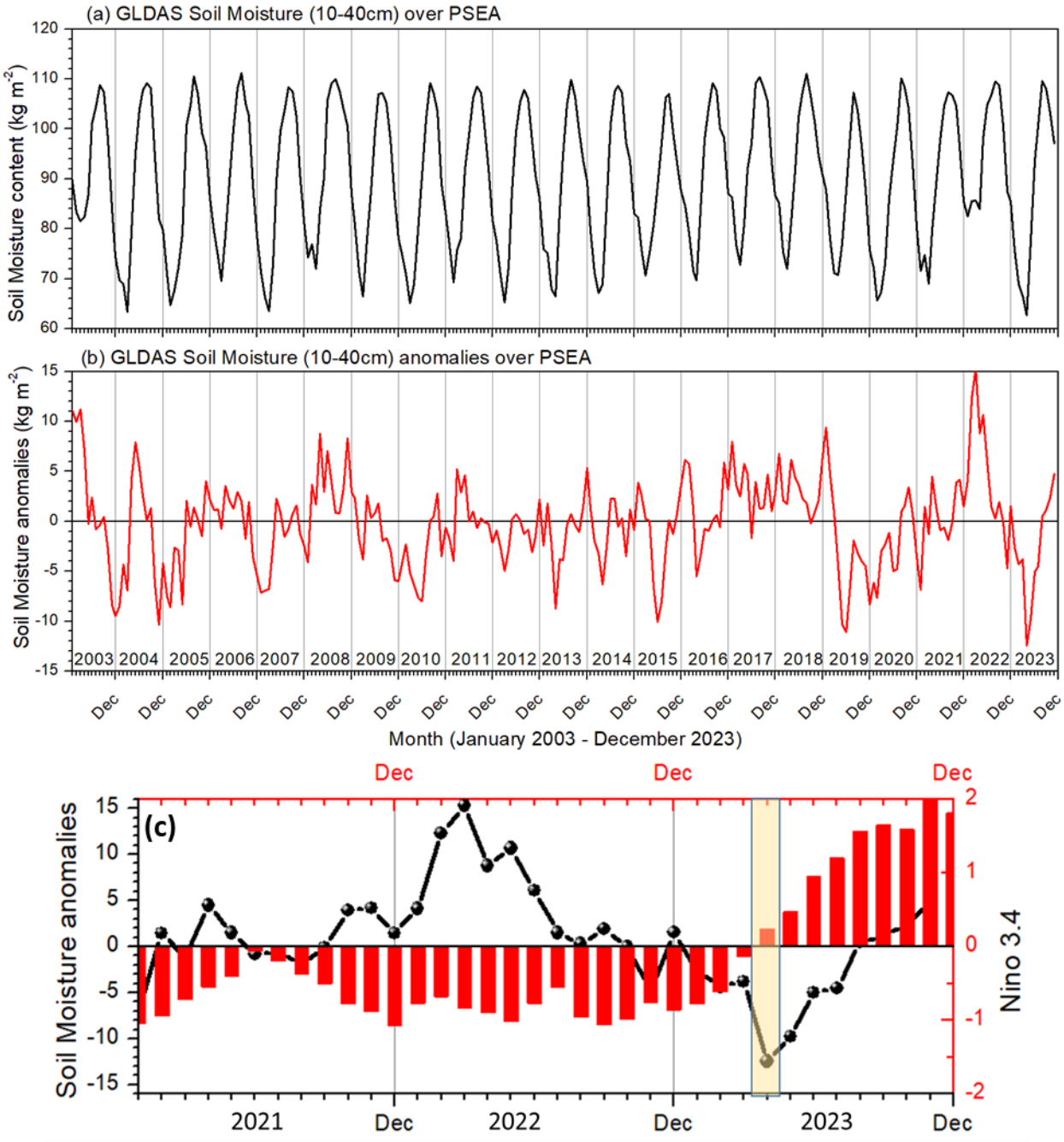

Sup. Figure 9. (a) Temporal variation of soil moisture (SM) content over northern Laos, (b) corresponding observed anomalies from January 2003 to December 2023. The evolution of SM anomalies (black) between January 2021 and December 2023, along with the evolution of Niño 3.4 Index (red bars). April 2023 was highlighted in sub plot (c).

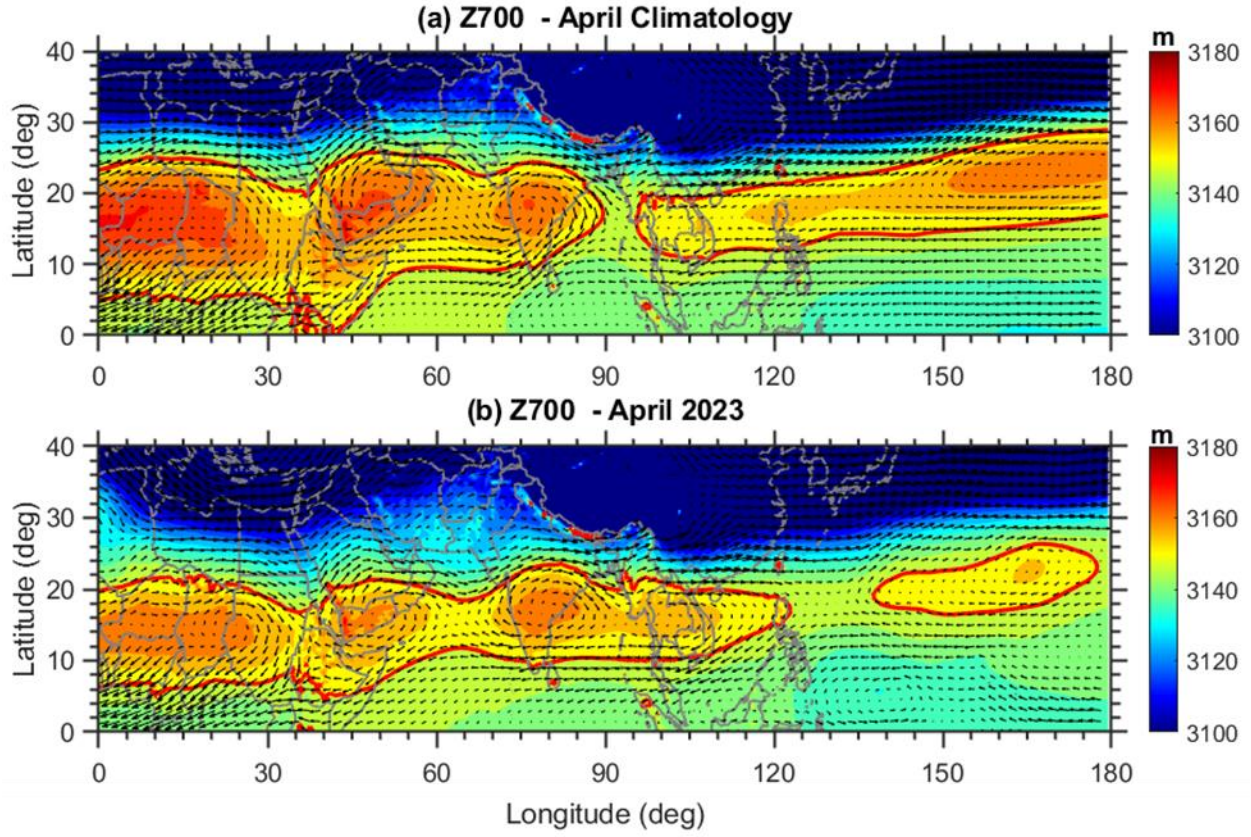

Sup. Figure 10. MERRA-2 reanalysis observed 700 hPa geopotential height (Z700) overlapped with the observed winds for (a) long-term April mean (2003-2023), (b) for April 2023.

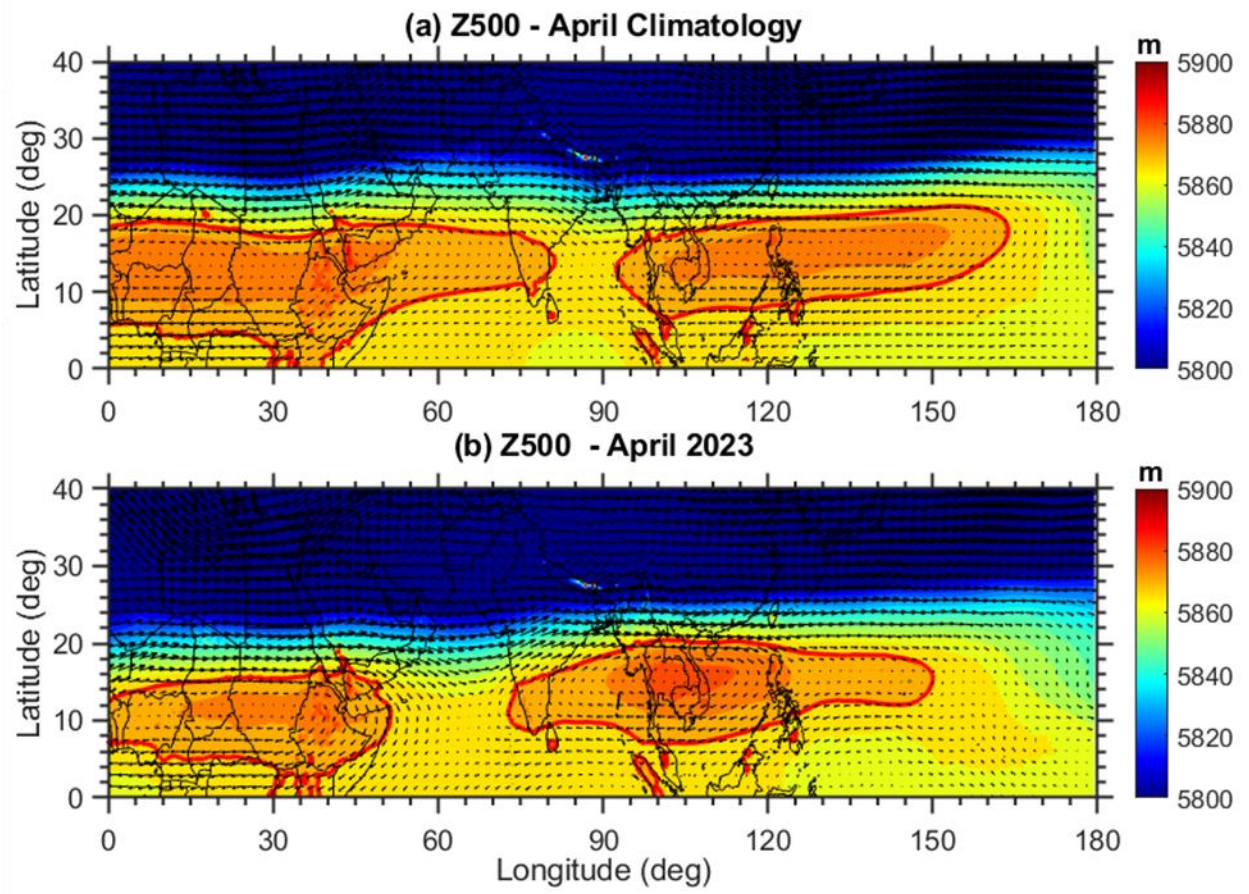

Sup. Figure 11. MERRA-2 reanalysis observed 500 hPa geopotential height (Z500) overlapped with the observed winds for (a) long-term April mean (2003-2023), (b) for April 2023.

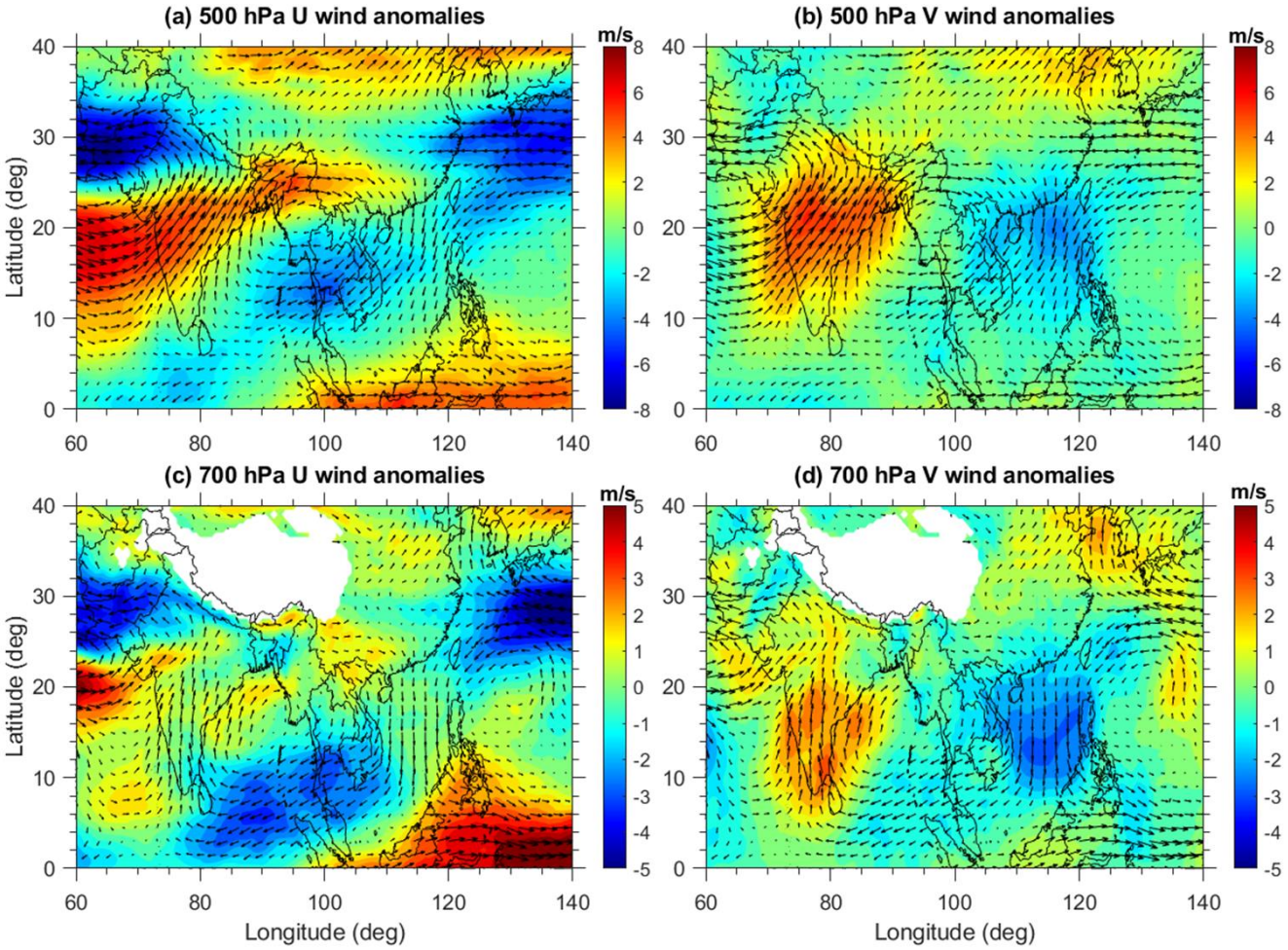

Sup. Figure 12. MERRA-2 reanalysis observed (a) 500 hPa zonal wind (U), (b) 500 hPa meridional wind (V) anomalies (color contours) overlapped with the observed wind vectors in April 2023. Subplots (c) and (d) are the same as (a) and (b), but observed at 700 hPa. The anomalies are calculated by subtracting the monthly mean of April 2023 from the April climatology for the period from 1991 to 2020.

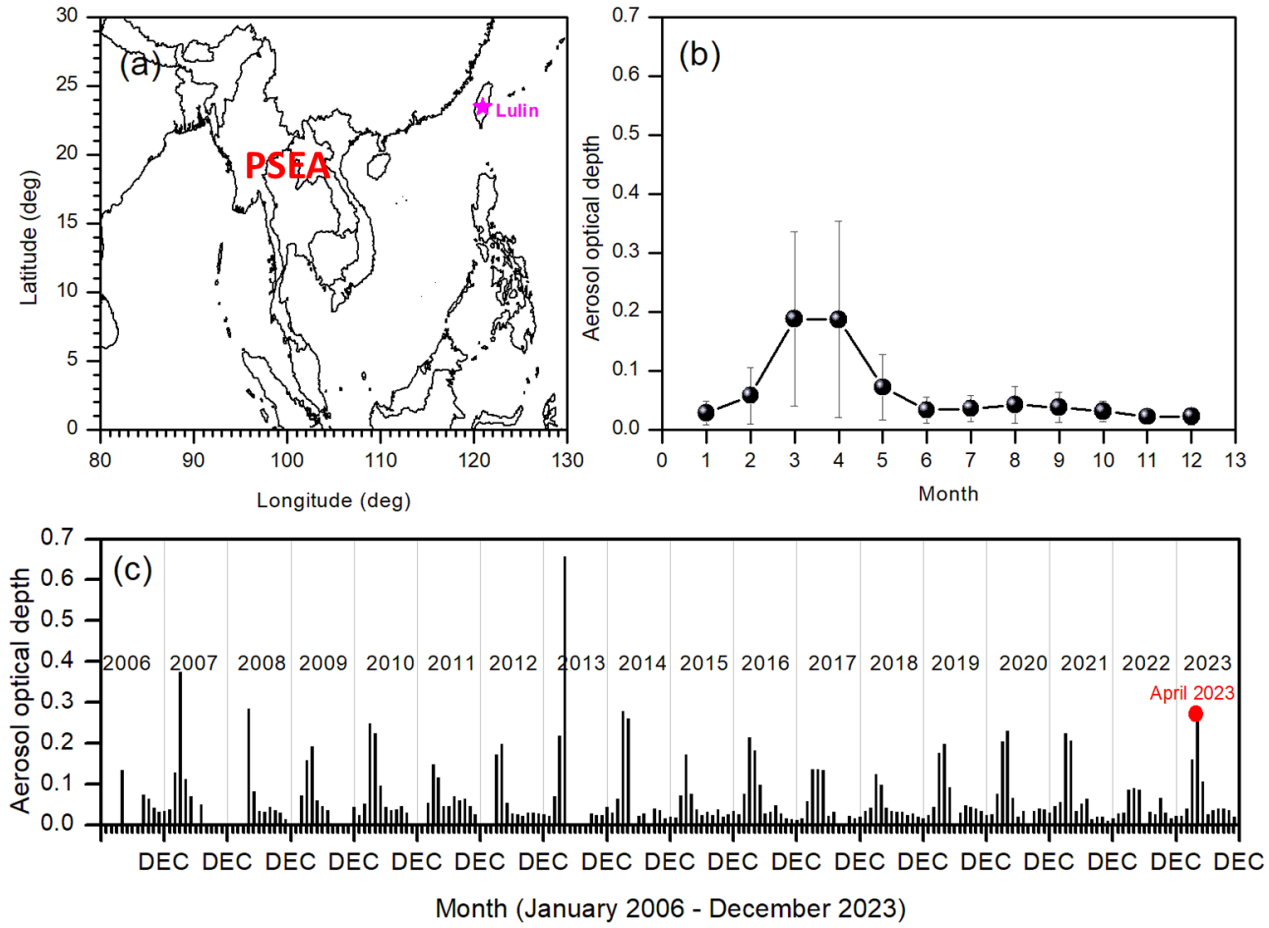

Sup. Figure 13. The location of the Lulin Atmospheric Background Station (LABS, 23°28′N, 120°52′E, 2,862 m) AERONET site (denoted by the purple star). (b) Monthly variations in aerosol optical depth (AOD) at Lulin. Vertical error bars represent the standard deviation from the mean. (c) Time series of monthly AOD values from January 2006 to December 2023.

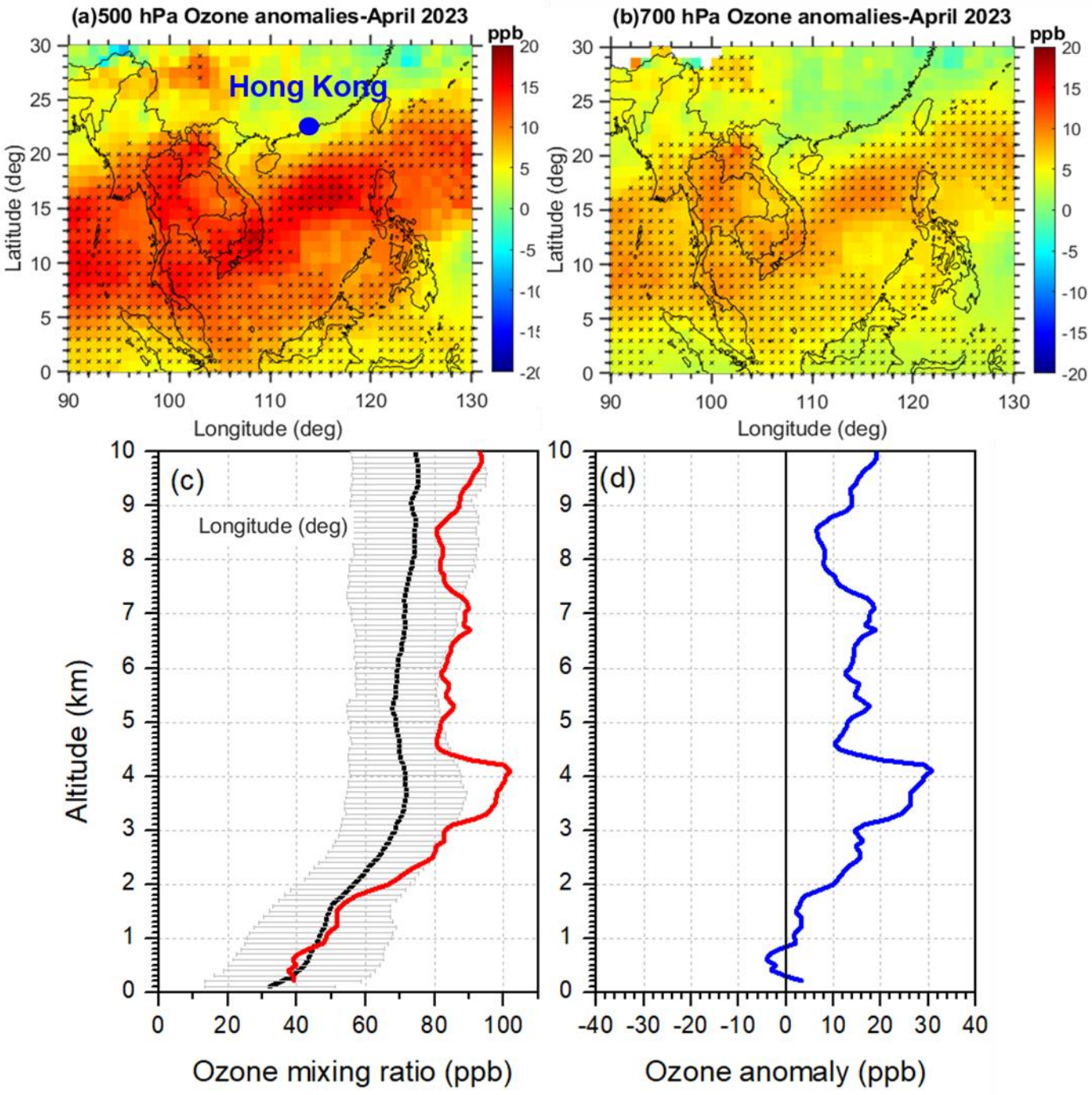

Sub. Figure 14. Spatial Distribution of AIRS satellite-measured Ozone Anomalies observed at (a) 500 hPa and (b) 700 hPa levels in April 2023. The regions marked with black hatches signify anomalies exceeding 2σ standard deviations from the long-term average for April, calculated from 2003 to 2022. The blue dot in subplot (a) indicates the position of the Hong Kong ozonesonde station. (c) The vertical profile of the monthly mean ozone mixing ratio obtained from the ozonesonde observations for April, comparing the long-term mean (black line) to the data from 2023 (red line), and (d) the percentage change in the ozone mixing ratio for April 2023 relative to the 2003-2022 long-term mean.

Sup. Table 1. MODIS total fire counts and the corresponding total accumulated fire radiative power (FRP) observed over peninsular Southeast Asia (PSEA) and each country within PSEA in April 2023. The percentage contribution of each country to the total fires and total FRP of PSEA is shown in the brackets, respectively.

Country	Total Fires	Fire Radiative Power (FRP)
PSEA	21198	2407283
Cambodia	242 (1.14%)	13402 (0.5%)
Laos	11877 (56.02%)	1530000 (63.5%)
Myanmar	7054 (33.27%)	777970 (32.32%)
Thailand	1322 (6.24%)	50276 (2.1%)
Vietnam	703 (3.32%)	35634 (1.5%)